

THE  $(\alpha, \alpha)$ ,  $(\alpha, \alpha')$  AND  $(\alpha, {}^3\text{He})$  REACTIONS ON  ${}^{12}\text{C}$  AT 139 MeVS. M. SMITH, G. TIBELL<sup>†</sup>, A. A. COWLEY<sup>††</sup>, D. A. GOLDBERG,H. G. PUGH, W. REICHART<sup>†††</sup> and N. S. WALL*Department of Physics and Astronomy, University of Maryland, College Park,  
Maryland 20742<sup>‡</sup>*

Received 2 March 1973

**Abstract:** The nucleus  ${}^{12}\text{C}$  was bombarded with 139 MeV  $\alpha$ -particles to study the characteristics of the elastic, inelastic, and  $(\alpha, {}^3\text{He})$  reactions. An optical model analysis of the elastic data yielded a unique family of Woods-Saxon potential parameters with central real well depth  $V \approx 108$  MeV, and volume integral  $J/4A \approx 353$  MeV  $\cdot$  fm<sup>3</sup>. By comparing the present results with those of other studies above 100 MeV, we find that the real part of the  $\alpha$ -nucleus interaction decreases with increasing energy; the fractional decrease with energy is roughly one-half that observed for proton potentials. Using the optical potential parameters derived from the elastic scattering, first-order DWBA calculations with complex first-derivative form factors reproduced the inelastic scattering data to the 4.44 MeV ( $2^+$ ) and 9.64 MeV ( $3^-$ ) states of  ${}^{12}\text{C}$ . For the  $0^+$  state at 7.65 MeV it was necessary to employ a real, second-derivative form factor to fit the data. The deformation lengths  $\beta_l R_m$  and deformations  $\beta_l$  obtained in this and other experiments are summarized and compared. DWBA calculations using microscopic model form factors were also performed for the  $2^+$  and  $3^-$  states using the wave functions of Gillet and Vinh Mau. These reproduced the shapes and relative magnitudes of the differential cross sections. We also fit the shape of the  $0^+$  differential cross section using a microscopic form factor which contains a node, which is similar to that occurring in the collective model second-derivative form factor. In the  $(\alpha, {}^3\text{He})$  reaction the differential cross sections to the ground state ( $\frac{1}{2}^-$ ) and the 3.85 MeV ( $\frac{3}{2}^+$ ) state in  ${}^{13}\text{C}$  could not be reproduced by zero-range local DWBA stripping calculations; it was necessary to employ finite-range and non-local corrections in the local-energy approximation. This DWBA analysis is notable in that unambiguous optical potentials were available for both entrance and exit channels. The ground state spectroscopic factor is in agreement with the prediction of Cohen and Kurath, while the relative spectroscopic factors agree fairly well with the rather few existing measurements of this kind.

E

NUCLEAR REACTIONS  ${}^{12}\text{C}(\alpha, \alpha)$ ,  $(\alpha, \alpha')$ ,  $(\alpha, {}^3\text{He})$ ,  $E = 139$  MeV, measured  $\sigma(E_\alpha, \theta)$ ,  $\sigma(E_{{}^3\text{He}}, \theta)$ .  ${}^{12}\text{C}$  deduced optical potential, inelastic transition strengths,  ${}^{13}\text{C}$  deduced spectroscopic strengths.

## 1. Introduction

The elastic and inelastic scattering of composite projectiles by nuclei has been studied quite extensively at energies below 100 MeV [ref. <sup>1)</sup>] and for several cases <sup>2–7)</sup> for  $\alpha$ -particles at energies over 100 MeV. The results are characterized, particularly for  $\alpha$ -particle projectiles, by the following familiar features:

<sup>†</sup> On leave from The Gustav Werner Institute, Uppsala, Sweden.

<sup>††</sup> On leave from CSIR, Pretoria, South Africa

<sup>†††</sup> On leave from the University of Zurich, Switzerland

<sup>‡</sup> Research supported in part by the US Atomic Energy Commission.

(a) The elastic differential cross sections are well reproduced by optical model calculations using a complex potential; at low energies a Woods-Saxon potential form with four free parameters is adequate, while at higher energies six free parameters appear necessary. At low energies the parameterizations suffer from both continuous and discrete types of ambiguity<sup>8)</sup>.

(b) For most inelastic transitions to collective states (vibrational or rotational), the experimental data are well reproduced by reaction calculations based on the collective optical model and the distorted-wave Born approximation (DWBA). The nuclear structure information (i.e., deformations, or deformation lengths) obtained from this type of analysis for a given target nucleus is generally found to be independent of the projectile type and incident energy.

The present experiment is a study of several of these features for the scattering by  $^{12}\text{C}$  of 139 MeV  $\alpha$ -particles. In particular, one purpose of this investigation was to test for a low  $A$ -nucleus, criteria recently developed by two of the present-authors<sup>2)</sup> for data necessary to resolve the discrete ambiguities in composite-projectile optical potentials. We sought to confirm an implication of ref. 2) that one should be able to eliminate the discrete ambiguity in the optical potential for a nucleus of a given  $A$  at a given incident energy, if, using that same energy, one has been able to eliminate the ambiguity for a nucleus of higher  $A$ , the absence of a discrete ambiguity in fitting the elastic scattering data of 139 MeV  $\alpha$ -particles by  $^{58}\text{Ni}$  was reported previously<sup>5)</sup>. We additionally sought to verify the criterion given in ref. 2) for the angular range of data necessary. To eliminate the ambiguity one must measure cross sections out to and beyond the semiclassically defined maximum deflection angle  $\Theta$ .

The incident energy of 139 MeV falls between the incident energies of two previous elastic  $\alpha$ -scattering investigations of  $^{12}\text{C}$ . The existence of  $\alpha$ -scattering data at 104 MeV [ref. 3)] and 166 MeV [ref. 4)] therefore also afforded us the opportunity of examining the energy dependence of the  $\alpha$ -nucleus interaction as characterized by the real part of the optical potential and comparing it with that of the proton-nucleus interaction.

We have also studied the inelastic transitions to the well-known<sup>9)</sup> collective states at 4.44 MeV ( $J^\pi = 2^+$ ) and 9.64 MeV ( $3^-$ ) in order to examine the adequacy of the description given above in (b) for intermediate energy inelastic scattering. The degree to which the collective optical model can describe such results above 100 MeV is not clear from previous studies; for example, the deformation parameters obtained at 166 MeV [ref. 4)] for these states are inconsistent with those extracted at lower energies and with other projectiles.

We also investigated the excitation of the  $J^\pi = 0^+$  state at 7.65 MeV. Some previous investigations<sup>10,11)</sup> appear to indicate that this state does not exhibit any simple collective character. We have employed a microscopic model analysis in addition to a collective model analysis in an effort to obtain some insight into the excitation of the  $0^+$  state. The effectiveness of the microscopic description for  $\alpha$ -particle inelastic scattering by  $^{12}\text{C}$  at these energies was examined by comparing microscopic

model predictions for the  $2^+$  and  $3^-$  states with the data. The results of these analyses are presented in sect. 4

In sect. 5 we discuss the results of the studies of the  ${}^{12}\text{C}(\alpha, {}^3\text{He}){}^{13}\text{C}$  reaction. Since very few such stripping reactions had been investigated at energies above 50 MeV, we were interested in assessing the ability to obtain spectroscopic information through DWBA calculations at such incident energies. The present analysis differs from previous cases in that unambiguous optical potentials are available for the  ${}^3\text{He}$  channel [ref <sup>12</sup>)] and, as a result of the present study, for the  $\alpha$ -channel

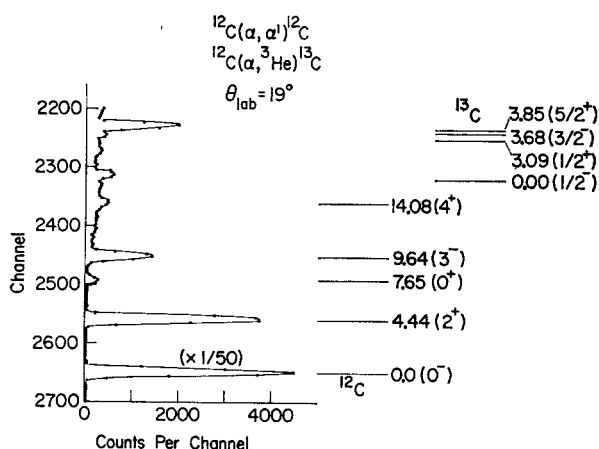


Fig 1 Energy spectrum for  ${}^4\text{He}$  and  ${}^3\text{He}$  particles observed at  $\theta_{\text{lab}} = 19^\circ$ .

## 2. Experimental techniques

The experiment was carried out using a 139 MeV  $\alpha$ -particle beam from the University of Maryland Cyclotron. The experimental apparatus, procedure and analysis were similar to that described <sup>5)</sup> previously. The target consisted of a  $0.88 \text{ mg/cm}^2$  CH foil. The measurements extended over an angular region from  $3.5^\circ$  to  $57.5^\circ$ (lab) with an incident beam intensity varying from a few nA at the smallest angles to 50 nA for the larger angles. The opening angle of the detector was  $0.5^\circ$ ; the total solid angle was  $1.4 \times 10^{-4} \text{ sr}$ . The uncertainty in the absolute cross sections is estimated to be 10 % and arises primarily from the uncertainty in the target thickness.

A typical spectrum energy is shown in fig. 1. Although no particle identification was employed it was still possible to distinguish between the peaks due to scattered  $\alpha$ -particles and those due to  ${}^3\text{He}$  particles by their kinematic variation with angle. The peaks from the  ${}^1\text{H}(\alpha, \alpha){}^1\text{H}$  and  ${}^1\text{H}(\alpha, {}^3\text{He}){}^2\text{H}$  reactions were used for determining the energy calibration and the accuracy of the angular settings <sup>5)</sup>. The average energy resolution was 400 keV (FWHM).

### 3. Elastic scattering

#### 3.1 OPTICAL POTENTIAL AMBIGUITIES

The elastic scattering data were analysed using a six-parameter optical potential of the Woods-Saxon form. The procedure employed has been described previously<sup>5)</sup>. Fig. 2 displays the elastic scattering data together with the results of the optical model calculations, table 1 lists the resulting optical potential parameters along with those obtained from elastic  $\alpha$ -scattering experiments on  $^{12}\text{C}$  at 104 MeV [ref. <sup>3)</sup>] and 166 MeV [ref. <sup>4)</sup>].

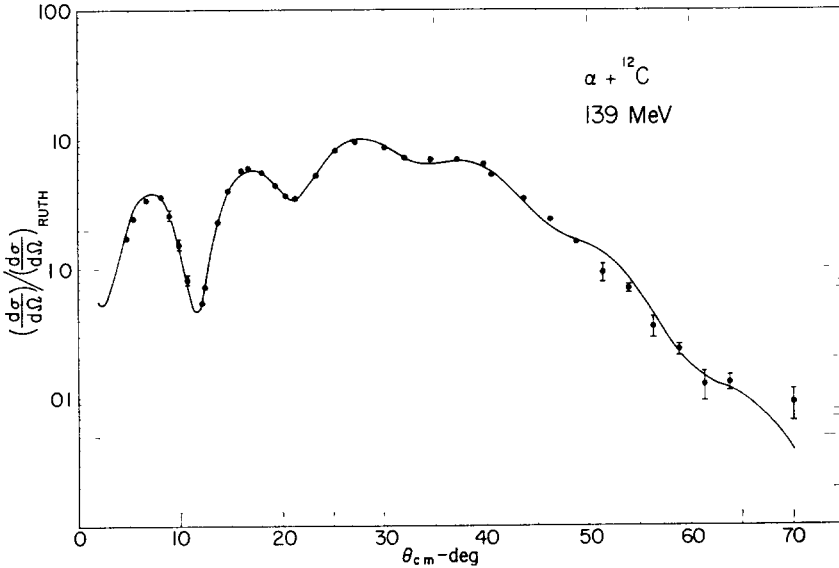


Fig. 2 The  $\alpha + ^{12}\text{C}$  elastic differential cross section as a ratio to Rutherford scattering. The curve is an optical model fit to the data obtained with the parameter set given in table 1. The error bars shown indicate the relative error in each point. Error bars less than 4% are not shown.

TABLE 1  
Optical potential parameters from elastic  $\alpha$ -scattering by  $^{12}\text{C}$  at incident energies  $E_\alpha$

$E_\alpha$ (MeV)	$V$ (MeV)	$R/A^{1/3}$ (fm)	$a$ (fm)	$W$ (MeV)	$R'/A^{1/3}$ (fm)	$a'$ (fm)	$\chi^2/f$	$J/4A$ MeV $\cdot$ fm <sup>3</sup>	Ref.
104	74.2	1.43	0.69	30.2	1.43	0.69	18.3	328	<sup>3)</sup>
104	114.0	1.22	0.80	13.8	1.91	0.50	7.9	393	<sup>a)</sup>
139	108.1	1.22	0.76	16.9	1.85	0.47	4.1	353	present work
166	85.0	1.34	0.70	17.7	1.77	0.52	13.0	324	<sup>4)</sup>
166	100.9	1.21	0.76	14.7	1.86	0.48	10.0	326	<sup>4)</sup>

The potential is given by  $U(r) = V_C(r) - Vf(x) - iWf(x')$ , where  $f(x) = (1 + e^x)^{-1}$ ,  $x = (r - R)/a$ ,  $x' = (r - R')/a'$ , and  $V_C(r)$  is the potential due to a uniformly charged sphere of radius  $R_C = 1.26 A^{1/3}$ . The eighth column lists the  $\chi^2$  values per degree of freedom; the ninth column gives the volume integral per interacting projectile-target nucleon pair for the real part of each potential.

<sup>a)</sup> Data from ref. <sup>3)</sup> reanalyzed with six free parameters, see text.

Before examining the results a brief discussion of the "uniqueness" of optical potentials may be in order. Several types of ambiguities in such potentials are known to occur within the constraint of a Woods-Saxon form. One of these is the discrete or phase ambiguity which gives rise to a set of potentials whose real well depths differ from one another by roughly 50 MeV [ref. <sup>8</sup>]. In addition, these individual potentials are themselves not "unique" but rather each represents a group or "family" of potentials, characterized by essentially identical volume integrals <sup>13)</sup> The real well parameters of potentials belonging to the same family generally obey a relation similar to  $VR^n = \text{const}$ . This type of parameter ambiguity within a family is frequently referred to as the continuous ambiguity.

In the present work only a single "family" was found which adequately described the data; the potential listed in table 1 represents the potential within that family which produced the lowest  $\chi^2$  per degree of freedom. As noted in the introduction, the absence of a discrete ambiguity in the present experiment for  ${}^{12}\text{C}$  is consistent with the prediction given in the paper by Goldberg and Smith <sup>2)</sup> based on a semiclassical description of the scattering. The incident energy is significantly above the critical energy or "triple point" energy  $E_{\text{crit}}$  given by <sup>2, 5)</sup>

$$E_{\text{crit}} = [U(r) + \frac{1}{2}r \frac{dU}{dr}]_{\text{max}},$$

where  $U(r)$  is the sum of the real nuclear plus Coulomb potentials, here,  $E_{\text{crit}}$  equals 32 MeV(lab).

The present results also support the criterion presented in ref. <sup>2)</sup> for the angular range of data required to eliminate the discrete ambiguity. For the potential listed in table 1 the semiclassically defined maximum deflection angle  $\Theta$  is about  $45^\circ$ . We observed that if we truncated the data employed in the optical potential search at an angle less than this, another potential family, with a deeper well depth ( $V \approx 206$  MeV,  $J/4A \approx 564$  MeV  $\cdot$  fm<sup>3</sup>) was found with an equivalent  $\chi^2$  per degree of freedom. However, if data to  $(\Theta + 10^\circ)$  were included in the search the  $\chi^2$  value for this deeper potential increased to a value which was a factor of ten over that for the shallower potential listed in table 1. These results are therefore similar to the  ${}^{58}\text{Ni}$  results presented in ref. <sup>2)</sup>.

Referring to table 1, it is seen that two potentials were quoted in the analysis of the 166 MeV data <sup>4)</sup>. These potentials appear to be an example of the continuous type of ambiguity, the potentials being two members of a single family: The real well depths of the two potentials differ by only about 15 MeV, whereas the different families are more typically on the order of 50 MeV apart; moreover, the volume integrals of the two potentials quoted differ by less than 1% <sup>†</sup>.

### 3.2 ENERGY DEPENDENCE OF THE POTENTIAL

In order to study the energy dependence of the  $\alpha$ - ${}^{12}\text{C}$  interaction as represented by the real part of the optical potential, we have examined the energy dependence of the

<sup>†</sup> Following the convention of ref. <sup>13)</sup> we quote the volume integral per projectile-target nucleon pair, which for  $\alpha$ -particles is given by  $J_\alpha = J/4A$ , rather than the volume integral  $J$ .

volume integral per projectile-target nucleon pair,  $J/4A$ . Weisser *et al.*<sup>13)</sup> demonstrated that this quantity remains fairly constant within a single family of parameters even though the parameters  $V$  and  $R$  vary considerably within the continuous ambiguity. The presence of many families of parameters for  $\alpha$ -particle optical potentials at lower energies, however, resulted in an uncertainty in the value of  $J/4A$  with which to characterize the real potential. This uncertainty has been eliminated with the resolution of the discrete ambiguity at the higher energies discussed here.

As may be seen from table 1, the volume integrals for the potentials obtained at 166 MeV and 104 MeV are both lower than that obtained in the present experiment. However, the 104 MeV data were originally analysed in a four-parameter model, in contrast to the six-parameter analysis used in the present work. In order to examine the energy dependence in a more consistent manner we performed a six-parameter analysis of the data given in ref. <sup>3)</sup>†. The value of  $J/4A$  obtained in this analysis is about 10 % higher than the value obtained for the 139 MeV data potential. The variation of the quantity  $J/4A$  over the energy range 104–166 MeV(lab) is consistent with a linear energy dependence. This linear decrease with energy is similar to that observed for proton optical potentials<sup>14,15)</sup>. One obtains a value of  $-1.1 \text{ MeV} \cdot \text{fm}^3/\text{MeV}$  for the slope of this decrease for  $\alpha$ -projectiles. Alternatively, if we write the volume integral for c.m. energy  $E_{\text{c.m.}}$  as

$$J_{\alpha}(E_{\text{c.m.}}) = J_{\alpha}(0)(1 + a_{\alpha} E_{\text{c.m.}}),$$

then  $a_{\alpha} = -0.0030 \text{ MeV}^{-1} \pm 20 \%$ .

It has often been suggested<sup>17)</sup> that the real well depths or strengths of  $\alpha$ -particle optical potentials at an energy  $E_{\text{c.m.}}$  are equal to four times those of nucleons at c.m. energy  $\frac{1}{4}E_{\text{c.m.}}$ . If this were true, or if even the  $\alpha$ -potential well depth was simply proportional to that of the proton potential, then the corresponding quantity  $a_p$  for protons should be approximately equal to  $a_{\alpha}$ . The energy dependence of the volume integrals for proton elastic data for  $^{40}\text{Ca}$  from 10–180 MeV was examined by Van Oers [ref. <sup>14)</sup>]. If we describe his results for protons using a relation similar to eq. (1), we find that  $a_p = -0.0048 \text{ MeV}^{-1}$ . In a more recent paper Humphreys<sup>16)</sup> investigated for many target nuclei and for energies up to 1 GeV the relation between the volume integrals ( $J/A$ ) for the real proton optical potentials and the quantity  $\gamma$ , where  $\gamma = (E + mc^2)/mc^2$ . Humphreys found that a linear dependence exists between  $J/A$  and  $\gamma^{-1}$  for  $E \leq 150 \text{ MeV}$ . This result can be approximated by a relation similar to eq. (1), with the result that  $a_p = -0.0056 \text{ MeV}^{-1}$ .

Keeping in mind that we are comparing volume integrals obtained from proton optical potentials for a variety of nuclei and over a rather large energy region with those resulting from  $\alpha$ -particle potentials for  $^{12}\text{C}$  between 104 and 166 MeV, it is noteworthy that  $a_p$  and  $a_{\alpha}$  are not approximately equal but differ by roughly a factor

† Hauser *et al.*<sup>3)</sup> report a better fit using a “wine-bottle” potential with seven free parameters. However, the  $\chi^2$  per degree of freedom for our six-parameter analysis of their data (7.9) was comparable to that of their seven-parameter analysis (7.1).

of two. Very recently the energy dependence of elastic  $\alpha$ -particle scattering from  ${}^{40}\text{Ca}$  was also studied by Lerner *et al.* <sup>18)</sup> between 40 and 115 MeV(lab) using a microscopic analysis. It was found there, too, that the variation with energy (c.m.) of the  $\alpha$ -particle real potential strength is one-half as rapid as that for protons, in agreement with the results reported here.

If one assumes that the energy dependence is due to an energy-independent non-local interaction of the Perey-Buck <sup>19)</sup> form, then the non-locality parameter value is related to  $a_x$  by <sup>18)</sup>

$$\beta_{NL}^2 = 2\hbar^2 a_x / M,$$

where  $M$  is the mass of the projectile. The value obtained ( $\approx 0.2$ ) equals that now conventionally employed in DWBA calculations for transfer reactions with non-locality corrections made in the local-energy approximation <sup>20)</sup>.

## 4. Inelastic scattering

### 4.1 THE $2^+$ AND $3^-$ STATES

In our study of the inelastic scattering to the first three <sup>9)</sup> excited states of  ${}^{12}\text{C}$ , i.e., the levels at 4.44 MeV ( $2^+$ ), 7.65 MeV ( $0^+$ ) and 9.64 MeV ( $3^-$ ), we analysed the results with DWBA calculations employing both collective optical model and microscopic model form factors. The collective model calculations used here are similar in procedure to those discussed in more detail in a previous article <sup>5)</sup> on  $\alpha$ -scattering at this energy. The form factors for a transition of multipolarity  $l$  are given by

$$F_l(r) = V(d/dr)f(x) + iW(d/dr)f(x') + F_l^C(r)$$

using the same notation as in table 1. The quantity  $F_l^C(r)$  is the Coulomb form factor [ref. <sup>21)</sup>]. Within this framework the shape of the theoretical differential cross section for a given  $l$  is almost completely determined at these energies once the optical potential parameters have been obtained from the analysis of the elastic scattering data. The nuclear structure information is contained in the deformation lengths  $\beta_l R_m$  which are given by

$$(\beta_l R_m)^2 = \frac{(d\sigma/d\Omega)_{\text{exp}}}{(d\sigma/d\Omega)_{\text{theory}}}.$$

The differential cross sections for the inelastic transitions are displayed in fig. 3. The experimental data for the  $2^+$  state obey the Blair phase rule <sup>22)</sup> fairly well, while the phase of the data for the  $3^-$  state is in between that of the  $2^+$  and the ground state. The solid curves in fig. 3 are the results of the collective model calculations. Although the second maximum for the  $3^-$  state is not reproduced satisfactorily, the theoretical predictions otherwise fit the  $2^+$  and  $3^-$  cross sections fairly well. The  $0^+$  state will be discussed in subsect. 4.2.

The values obtained for  $\beta_l R_m$  from the present data are listed in table 2 along with previously published results for  $\beta_l R_m$  and  $\beta_l$  obtained from collective model analyses.

We have indicated in this table the quantity (either  $\beta_i$  or  $\beta_i R_m$ ) which was quoted in the original reports. We attempted to normalize the results to the type of calculation performed for the present data, namely one which employs a complex form factor in which it has been assumed that  $\beta_i R$  for the real potential equals  $\beta'_i R'$  for the imagi-

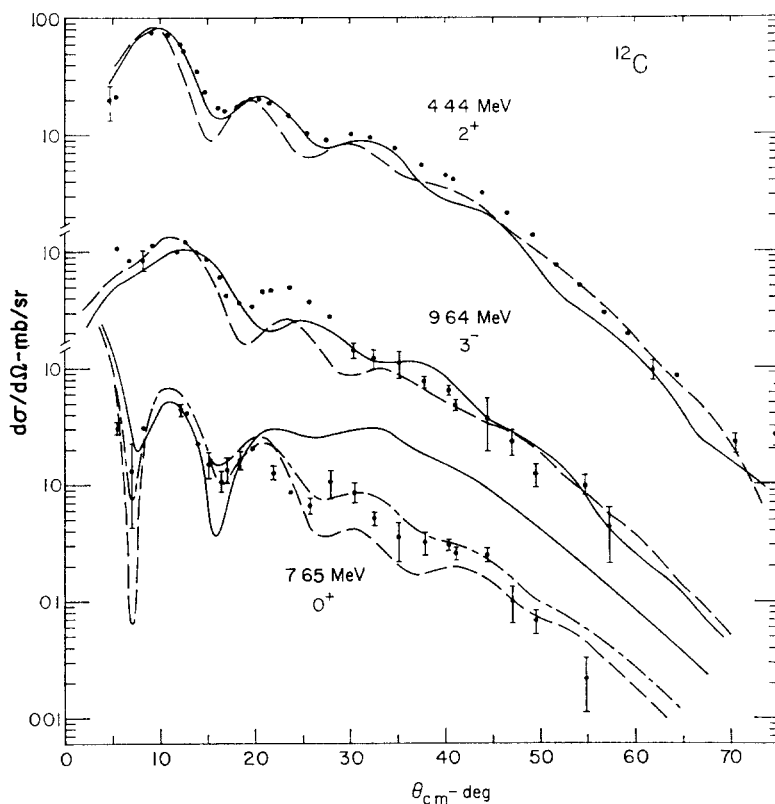


Fig 3 Differential cross sections for the 4.44 MeV ( $J^\pi = 2^+$ ), 9.46 MeV ( $3^-$ ) and 7.65 MeV ( $0^+$ ) levels in  $^{12}\text{C}$ . The curves are the results of first-order DWBA calculations (see text). The solid curves were obtained with collective model form factors of a complex first-derivative form, the dashed-dot curve for the 7.65 MeV level was obtained with a second-derivative form factor. The dashed curves are the results of microscopic model calculations; they have been arbitrarily normalized to the data (see text).

nary potential, rather than  $\beta_i = \beta'_i$ . This necessitated, for example, multiplying published  $\beta_i$  values by the factor  $R(1 + W^2/V^2)^{-\frac{1}{2}}$  to obtain  $\beta_i R_m$  for cases in which only a real form factor was employed and in which  $R' = R$  and  $a' = a$ . In some cases where  $R' \neq R$  or  $a' \neq a$ , a value for  $\beta_i R_m$  could not be derived from the published values for  $\beta_i$ .

As can be seen from table 2 the values of  $\beta_2 R_m$  all fall, with the exception of the 42 MeV  $\alpha$ -values, within  $\pm 20\%$  of  $\beta_2 R_m = 1.4$ . The values for  $\beta_2$  appear to be



clustered around  $0.60 \pm 10\%$  and  $0.47 \pm 10\%$ , while the values for  $\beta_3$  are clustered around  $0.42 \pm 20\%$  and  $0.20 \pm 20\%$ . Although differences in the quality of fits and type of analyses in the different investigations prevent any strong conclusions from being drawn, these results suggest that there is a correlation between the type of pro-

TABLE 2  
Summary of inelastic scattering results for the lowest  $2^+$  and  $3^-$  states of  ${}^{12}\text{C}$

Exp.	Inc energy (MeV)	$\beta_2$ <sup>a)</sup>	$\beta_2 R_m$ <sup>a)</sup> (fm)	$\beta_3$ <sup>a)</sup>	$\beta_3 R_m$ <sup>a)</sup> (fm)	Ref.
(p, p')	40	0.60	1.68 <sup>b)</sup>	0.44	1.23 <sup>b)</sup>	<sup>a)</sup>
(p, p')	46	0.61 <sup>c)</sup>	1.64 <sup>c)</sup>	0.41 <sup>c)</sup>	1.12 <sup>c)</sup>	<sup>10)</sup>
(p, p')	155	0.67		0.57		<sup>b)</sup>
(d, d')	52	0.57	1.66	0.37	1.06 <sup>b)</sup>	<sup>28)</sup>
(d, d')	70	0.47	1.12	0.27	0.65	<sup>1)</sup>
(d, d')	80	0.47		0.35		<sup>35)</sup>
( ${}^3\text{He}$ , ${}^3\text{He}'$ )	100	0.51 <sup>d)</sup>	1.25	0.30 <sup>d)</sup>	0.75	<sup>12)</sup>
( $\alpha$ , $\alpha'$ )	42	0.48 <sup>e)</sup>	1.97 <sup>e)</sup>			
( $\alpha$ , $\alpha'$ )	139	0.46 <sup>d)</sup>	1.27	0.24 <sup>d)</sup>	0.68	present results
( $\alpha$ , $\alpha'$ )	166	0.30		0.18		<sup>6)</sup>
( ${}^{12}\text{C}$ , ${}^{12}\text{C}'$ )	127	0.62 <sup>f)</sup>	1.50 <sup>b, f)</sup>			<sup>j)</sup>
( ${}^{16}\text{O}$ , ${}^{16}\text{O}'$ )	168	0.54 <sup>f)</sup>	1.47 <sup>b, f)</sup>			<sup>j)</sup>

Listed are the present and previously published results for the deformations  $\beta_i$  and deformation lengths  $\beta_i R_m$  obtained from analyses employing the collective optical model in DWBA calculations.

<sup>a)</sup> Values as published unless noted otherwise.

<sup>b)</sup> Obtained from  $\beta_i$  by multiplying by  $R$ .

<sup>c)</sup> Average value of published results.

<sup>d)</sup> Obtained by dividing  $\beta_i R_m$  by  $R$ .

<sup>e)</sup> It is unknown whether a real or complex form factor was employed.

<sup>f)</sup> Published values multiplied by  $(1 + W^2/V^2)^{-1/2}$ .

<sup>a)</sup> M. P. Fricke and G. R. Satchler, Phys. Rev. **139** (1965) B567.

<sup>b)</sup> R. M. Haybron, Nucl. Phys. **79** (1966) 33.

<sup>1)</sup> G. H. Harrison, thesis, University of Maryland, 1972, unpublished.

<sup>j)</sup> R. H. Bassel, G. R. Satchler and R. M. Drisko, Nucl. Phys. **89** (1966) 419.

jectile and the  $\beta_i$  values. The nucleon and heavy-ion inelastic scattering results cluster around the higher values, while the light composite projectile results cluster about values roughly 25% lower.

The results of other investigations employing either different types of projectiles or analyses span the range of values presented here. The  $\beta_2$  values obtained from analyses <sup>23)</sup> of  $(\pi, \pi')$  experiments at energies from 120 to 280 MeV are 0.47 to 0.62. Inelastic electron scattering studies at 300 MeV [ref. <sup>24)</sup>] have obtained values of  $\beta_2 R_m$  of 2.0 and  $\beta_2$  values of 0.52 to 0.63 in the nuclear surface. A Blair-Austern coupled-channel analysis <sup>6)</sup> of 104 MeV  $\alpha$ -data indicates that  $\beta_2 = 0.29$ .

#### 4.2 THE $0^+$ STATE AT 7.65 MeV

Compared to the  $2^+$  and the  $3^-$  states at 4.44 MeV and 9.64 MeV the  $0^+$  state of  ${}^{12}\text{C}$  at 7.65 MeV is less well understood. Several different reaction models have not

been very successful, for instance, in describing its excitation by inelastic proton or  $\alpha$ -scattering. For 45 MeV protons Satchler<sup>10)</sup> obtained a relatively good fit to the experimental data only by assuming that the  $0^+$  state was reached through a multiple excitation process involving the  $2^+$  state at 4.44 MeV. At 185 MeV [ref. 11)] simplified distorted wave calculations adequately describe the inelastic proton scattering results for the strongly excited collective states, but fail to describe the angular distribution observed for the  $0^+$  state.

Our experimental results for the  $0^+$  state are shown in fig. 3 together with curves calculated in the DWBA. As can be seen from the figure, it was not possible to obtain a good fit using the same prescription as that used for the  $2^+$  and  $3^-$  states. Instead of a first-derivative complex form factor it was necessary to use a second derivative form; we also found that a slightly better fit was obtained if only the real part was used. The main difference between a first and second-derivative  $l = 0$  form factor is, of course, that the latter contains a node in the surface region. As discussed at some length by Satchler<sup>10)</sup> in his analysis of 45 MeV proton scattering data, such a node can be obtained, and the need for it interpreted, in many ways within the framework of the collective optical model. In an attempt to obtain more direct insight into the structure of this state and its excitation, we performed DWBA calculations using microscopic model form factors.

#### 4.3. MICROSCOPIC MODEL ANALYSIS

The framework of the particular microscopic model employed here is described in some detail in ref. 25). The form factors were calculated with the computer program ATHENA IV [ref. 25)]. An effective  $\alpha$ -nucleon interaction with Gaussian shape was employed which has a range of 2.0 fm and a depth of 37 MeV. This interaction has been employed successfully in fitting the forward angle pattern of elastic differential cross sections<sup>26)</sup>. The ability of such microscopic model calculations to describe the inelastic  $\alpha$ -scattering at these energies was tested by performing calculations for the strong collective  $2^+$  and  $3^-$  states. In calculating form factors for these states we employed the amplitudes of the random phase approximation wave functions determined by Gillet and Vinh Mau<sup>27)</sup> (approximation II). The radial parts of the particle (hole) wave function were calculated by solving the Schrodinger equation for a Woods-Saxon potential<sup>†</sup>; the depth of the potential was adjusted to produce the appropriate binding energies. Unbound particle states were arbitrarily treated as slightly bound. The cross sections obtained for the  $2^+$  and  $3^-$  states were not very sensitive to the exact value of the binding energy. The resulting microscopic model predictions are shown as dashed lines in fig. 3. As may be seen the shapes of the differential cross

<sup>†</sup> A potential of the form

$$-V(r) = V_0 f(y) + I \cdot s V_{s0} (1/r) df(y)/dr$$

was employed, where

$$f(y) = 1 + e^y, \quad y = (r - R_0)/a, \quad R_0 = 1.25 A^{1/3}, \\ a = 0.5 \text{ fm}, \quad V_{s0} = 0.2 V_0 \text{ MeV}.$$

sections for the  $2^+$  and  $3^-$  states are adequately described by the predictions. Although the relative magnitudes of the  $2^+$  and  $3^-$  cross sections are reproduced well, the absolute magnitudes, however, are a factor of two too small; the curves have been multiplied by 2 to match the data.

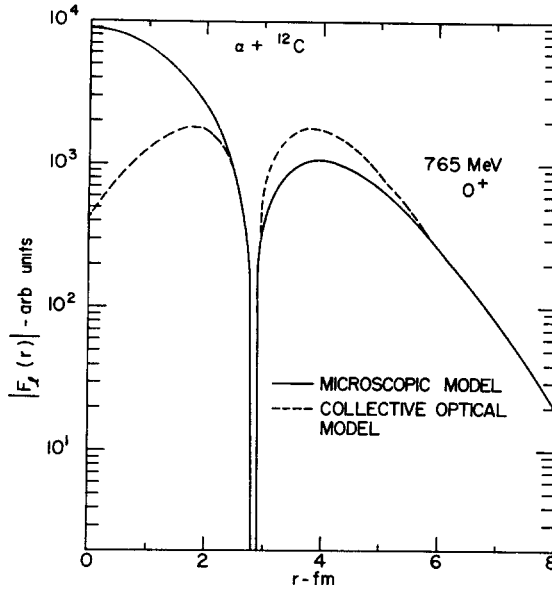


Fig. 4. Comparison of the second-derivative collective model form factor and the microscopic model form factor for the 765 MeV level.

Satisfied with the ability of the microscopic model calculations to describe at least the shape and *relative* magnitudes of the  $2^+$  and  $3^-$  collective states we investigated the description of the  $0^+$  state. Following the procedure employed by Hinterberger *et al.* <sup>28)</sup> to fit the  $(d, d')$  data for this state, we attempted to describe the  $0^+$  state in terms of the following particle-hole wave function:

$$\Psi(0^+) = 0.84(1p_{\frac{1}{2}}^{-1}2p_{\frac{1}{2}}) + 0.55(1s_{\frac{1}{2}}^{-1}2s_{\frac{1}{2}}).$$

The resulting cross section prediction is shown in fig. 3. The shape of the angular distribution resembles the measured differential cross section fairly well. (The curve has been normalized to the collective model curve near  $11^\circ$ ). The similarity of the second derivative collective model prediction and the microscopic model prediction can be ascribed to the similarity in the shapes of their form factors, which are shown in fig. 4. Both form factors exhibit a node at the same place in the nuclear surface.

In order to normalize the microscopic prediction we reduced the predicted cross sections by roughly a factor of 1.25 (as compared to the factor of 2 for the  $2^+$  and  $3^-$

states). Although the binding energies chosen for the unbound particle configurations significantly affect the cross section in this case, we can conclude that excitation of particle-hole configurations of the above type could account for the excitation of the  $0^+$  state.

### 5. The $^{12}\text{C}(\alpha, ^3\text{He})^{13}\text{C}$ reaction

In the recorded spectra we could identify and analyse, through most of the angular region studied, two peaks due to  $^3\text{He}$  particles from the  $^{12}\text{C}(\alpha, ^3\text{He})^{13}\text{C}$  reaction. The peaks correspond to the production of the  $^{13}\text{C}$  ground state ( $J^\pi = \frac{1}{2}^-$ ) and the  $\frac{5}{2}^+$  state<sup>29</sup>) at 3.85 MeV. (See fig. 1.) The differential cross sections are shown in

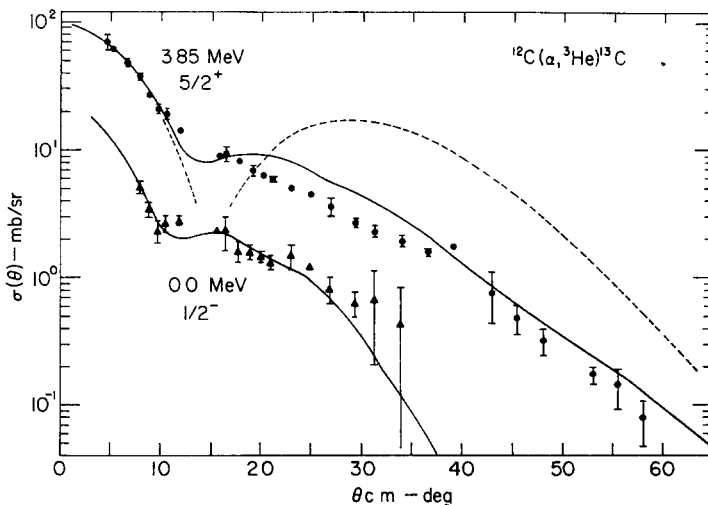


Fig. 5. Differential cross sections for the 0.0 MeV ( $\frac{1}{2}^-$ ) and 3.85 MeV ( $\frac{5}{2}^+$ ) levels of  $^{13}\text{C}$  observed via the  $^{12}\text{C}(\alpha, ^3\text{He})^{13}\text{C}$  reaction. The curves are DWBA predictions with (—) and without (---) finite-range, non-local corrections made in the local-energy approximation.

fig. 5 together with DWBA curves. Possible contaminations to the differential cross section measured for the 3.85 MeV state due to contributions from the known<sup>29</sup>)  $\frac{3}{2}^-$  level at 3.68 MeV are considered negligible; the excitation energy (3.85 MeV) obtained from the observed peak position remained constant over the entire angular region to within a value which is small compared to the separation of the 3.68 and 3.85 MeV levels.

The DWBA analysis reported here differs from previous such analyses of ( $^3\text{He}, \alpha$ ) reactions<sup>17, 30, 31</sup>) in that unambiguous optical model parameters were available for both the incident and exit channels. The entrance channel parameters were those obtained in the present scattering study, while the exit channel parameters we employed were obtained from a recent study of  $^3\text{He}$  scattering by  $^{12}\text{C}$  at 100 MeV [ref. 12)]. As in the present elastic scattering investigation only a single family of parameters

was found to fit the  ${}^3\text{He}$  data, which extended out to and beyond the semiclassically defined maximum deflection angle. Previously reported analysis of the  ${}^{12}\text{C}({}^3\text{He}, \alpha)$  reaction at 56 MeV [ref. <sup>30</sup>)] and 104 MeV [ref. <sup>31</sup>)] were hampered by the ambiguities and uncertainties in the optical model parameters.

Both zero-range, local (ZRL) and finite range, non-local (FRNL) DWBA calculations were investigated. The FRNL calculations were performed via corrections made in the local-energy approximation <sup>32</sup>) to the ZRL form factor. For the ZRL form factor we employed the wave function of a neutron bound in a Woods-Saxon potential with parameter values of  $R/A^{1/3} = 1.25$  fm, and  $a = 0.65$  fm; the well depth was varied to produce the correct binding energy. A Thomas-type spin-orbit potential was also included with a strength parameter of 25.

The result of the ZRL calculation for the 3.85 MeV level is shown in fig. 5 as a dashed curve. The ZRL result for the ground state is similar in shape and thus is not shown. Both curves produce unsatisfactory fits to the data. The solid curves shown in fig. 5 are the results of the FRNL calculations. The non-local corrections to the  ${}^3\text{He}$  and  $\alpha$ -particle channels affected the cross sections little. The major variation which produced the very satisfactory fits was obtained with the inclusion of the finite-range corrections. We used non-local parameter values of 0.2 fm for both channels and a range parameter of 1.75 fm. These values are typical of the values previously employed in analyses of this type <sup>17</sup>). The latter value produced the best fits to the differential cross sections of both levels. The finite-range correction was normalized to 1.0 at large values of  $r$ .

Absolute spectroscopic factors were obtained by normalizing the calculations with a previously obtained value <sup>17</sup>) for the absolute normalization constant,  $D_0^2 = 23 \text{ MeV} \cdot \text{fm}^3$ , with the DWBA code TANYA <sup>33</sup>). For  $(\alpha, {}^3\text{He})$  reactions spectroscopic factors  $S_{ij}$  are given by

$$NS_{ij} = \frac{2J_i + 1}{2J_f + 1} \frac{(d\sigma/d\Omega)_{\text{exp}}}{(d\sigma/d\Omega)_{\text{DWBA}}},$$

where  $N = (2s_b + 1)D_0^2/(2s_a + 1) = 46 \text{ MeV} \cdot \text{fm}^3$ . We find that  $S_{\frac{1}{2}}(\text{g.s.}) = 0.69 \pm 15\%$  and  $S_{\frac{3}{2}}(3.85 \text{ MeV}) = 0.40 \pm 15\%$ . The errors are indicative of only the uncertainties in the data and the matching of the DWBA curve to the data.

The ground state value agrees well with that predicted by Cohen and Kurath <sup>34</sup>) and with the  $(\alpha, {}^3\text{He})$  results at 104 MeV [ref. <sup>31</sup>)] and the  $(d, p)$  results of Duhamel *et al.* <sup>35</sup>). The relative spectroscopic factor of the 3.85 MeV level to that of the ground state is  $S_{\frac{3}{2}}/S_{\frac{1}{2}} = 0.6$ .

Depending on which potential they used in their distorted-wave analysis Glover and Jones <sup>36</sup>) found values in the range 0.7–1.1 from  $(d, p)$  and 0.8 from  $(t, d)$  reactions for the relative spectroscopic factor of the  $\frac{3}{2}^+$  state transition as compared to the ground state transition. At 80 MeV Duhamel *et al.* <sup>33</sup>) report a value close to 1.0, which was extracted under the assumption that the contribution from transitions to the 3.68 MeV state corresponds to a spectroscopic factor in agreement with the calcula-

tions by Cohen and Kurath<sup>34</sup>). The present results are thus consistent within the stated errors with spectroscopic factors obtained from other reactions.

## 6. Conclusions

In our investigation of the scattering of  $\alpha$ -particles by  $^{12}\text{C}$  we have found that the elastic differential cross section is well reproduced by optical model calculations using a six-parameter Woods-Saxon complex potential. The data satisfy the criteria developed by Goldberg and Smith<sup>2</sup>) for the incident energy and angular range of data required to eliminate the discrete ambiguity in the real part of the potential. As predicted, only a single family of parameters was found which produced a fit to the data. Also borne out is the assertion that if the ambiguity has been eliminated for one nucleus at a given energy, then using the same incident energy one can expect to be able to eliminate the ambiguity in the optical potential for a nucleus with lower  $A$ .

With the ability to obtain at intermediate energies unambiguous potentials for alpha particles and other composite projectiles, one can begin to examine the energy dependence of the projectile-nucleus interaction. We have found for a small sample of data that the  $\alpha$ -nucleus interaction, as characterized by the real part of the optical potential, decreases with energy one-half as rapidly as the proton-nucleus interaction. This difference in energy dependence is not yet fully understood. It does appear to indicate, however, that the strengths of the real part of the  $\alpha$ -particle optical potentials are not equal to the nuclear strengths at one-fourth the energy.

We find that in our study of the inelastic transitions, DWBA calculations with either macroscopic or microscopic model form factors are able to reproduce the shapes of the differential cross sections. For the  $0^+$  state at 7.65 MeV, it was necessary that the form factor contain a node, which is obtained in the collective model by employing a second-derivative form factor. A comparison has been made of published deformations and deformation lengths  $\beta_1 R_m$  obtained via DWBA calculations, for the 4.44 MeV ( $2^+$ ) and 9.64 MeV ( $3^-$ ) levels. In general, the values deviate from one another to a greater degree than values similarly obtained for heavier nuclei<sup>26</sup>). The results appear to indicate that values obtained using composite projectiles are systematically 25 % lower than those obtained using nucleons. For this light nucleus, this effect and the spread of values may be due to the neglect of exchange contributions, or the neglect of the strong coupling to other states in this type of analysis.

It appears from our study of the ( $\alpha$ ,  $^3\text{He}$ ) reaction, that one could successfully employ this reaction at intermediate energies to obtain spectroscopic information, if the incident and exit optical potentials have been determined unambiguously. Since there is essentially no angular momentum mismatch for the levels studied due to the large  $Q$ -value, the partial waves contributing significantly to the cross sections were determined by the elastic scattering measurements<sup>17</sup>). We find, however, that finite-range corrections must be included in order to reproduce the data. These corrections are large since the difference in the potentials ( $V_\alpha - V_{^3\text{He}} - V_n$ ) is not approximately

zero. Further study of this type of reaction appears necessary at energies where unambiguous potentials are available.

The stay at the University of Maryland for one of the authors (G.T.) was made possible through a grant from the Sweden-American Foundation as well as through support from the Swedish Atomic Research Council and the University of Maryland. The financial support from the South African Council for Scientific and Industrial Research as well as from the University of Maryland is acknowledged by another author (A.A.C.).

### References

- 1) P E Hodgson, Nuclear reactions and nuclear structure (Clarendon Press, Oxford, 1971)
- 2) D A Goldberg and S M. Smith, Phys. Rev Lett **29** (1972) 500
- 3) G Hauser, R. Lohken, H. Rebel, G. Schatz, G W. Schweimer and J. Specht, Nucl. Phys **A128** (1969) 81, and references therein
- 4) B Tatischeff and I. Brissaud, Nucl Phys **A155** (1970) 89
- 5) D A. Goldberg, S M Smith, H G Pugh, P. G. Roos and N S. Wall, Phys. Rev C, to be published
- 6) J. Specht, G W Schweimer, H Rebel, G. Schatz, R Lohken and G Hauser, Nucl. Phys **A171** (1971) 65
- 7) H H. Duham, Nucl Phys **A118** (1968) 563
- 8) R M Drisko, G R Satchler and R H Bassel, Phys. Lett. **5** (1963) 347,  
D F Jackson and C G Morgan, Phys. Rev. **175** (1968) 1402, and references therein
- 9) F. Ajzenberg-Selove and T Lauritsen, Nucl Phys **A114** (1968) 1
- 10) G R Satchler, Nucl Phys. **A100** (1967) 497
- 11) O. Sundberg and G Tibell, Ark Fys **39** (1969) 397,  
G. Tibell, report GWI-PH 7/70, Gustav Werner Institute, unpublished
- 12) D A. Goldberg, S M Smith and H D. Holmgren, Bull. Am Phys. Soc **17** (1972) 896
- 13) D. C. Weisser, J S Lilley, R K Hobbie and G W Greenlees, Phys. Rev. C **2** (1970) 544, and references therein
- 14) G. W. Greenlees, G J Pyle and Y C Tang, Phys Rev **171** (1968) 1115
- 15) W T. H. van Oers, Phys Rev. C **3** (1971) 1550
- 16) R. Humphreys, Nucl Phys **A182** (1972) 580
- 17) R Stock, R. Bock, P David, H H Duham and T. Tamura, Nucl. Phys **A104** (1967) 136
- 18) G M. Lerner, J C Hiebert, L L Rutledge, Jr., and A M Bernstein, Phys Rev C **6** (1972) 1254
- 19) F G Perey and B Buck, Nucl Phys **32** (1962) 353
- 20) F G Perey and D S. Saxon, Phys. Lett **10** (1964) 107
- 21) R H. Bassel, G R Satchler, R M. Drisko and E Rost, Phys Rev. **128** (1962) 2693
- 22) J S Blair, Phys Rev **115** (1959) 928
- 23) G W. Edwards and E. Rost, Phys Rev. Lett **26** (1971) 785, and erratum **26** (1971) 1354
- 24) A Nakada, Y. Torizuka and Y. Horikawa, Phys Rev. Lett. **27** (1971) 745
- 25) G R Satchler, Nucl Phys. **77** (1966) 481; **A95** (1967) 1;  
M B Johnson, L W. Owen and G R. Satchler, Phys Rev. **142** (1966) 748,  
F S Chwieroth, J I. Dodson, M B Johnson, L W. Owen and G. R Satchler, Oak Ridge Technical Report number TM-2703 (1969) unpublished
- 26) A. M Bernstein, Advances in nuclear physics **3** (1969) 325
- 27) V Gillet and N Vinh Mau, Nucl Phys. **54** (1964) 321
- 28) F. Hinterberger, G Mavile, U Schmidt-Rohr, G J Wagner and P Turek, Nucl Phys **A115** (1968) 570
- 29) F Ajzenberg-Selove, Nucl Phys **152** (1970) 1
- 30) P Gaillard, R Bouché, L. Feuvrais, M Gaillard, A Guichard, M Gusakow, J L. Leonhardt and J R Pizzi, Nucl Phys **A131** (1969) 353

- 31) G. Hauser, R. Lohken, G. Nowicki, H. Rebel, G. Schatz, G. Schweimer and J. Specht, Nucl. Phys. **A182** (1972) 1
- 32) F. G. Perey, in Proc. Conf. on direct interactions and nuclear reaction mechanisms, Padua, 1962 (Gordon and Breach, New York, 1963);  
P. J. A. Buttle and L. J. B. Goldfarb, Proc. Phys. Soc. **83** (1964) 701;  
J. K. Dickens, R. M. Drisko, F. G. Perey and G. R. Satchler, Phys. Lett. **15** (1965) 337
- 33) T. Provost and S. M. Smith, private communication
- 34) S. Cohen and D. Kurath, Nucl. Phys. **A101** (1967) 1
- 35) G. Duhamel, L. Marcus, H. Langevin-Johot, J. P. Didelez, P. Narboni and C. Stephan, Nucl. Phys. **A174** (1971) 485
- 36) R. N. Glover and A. D. W. Jones, Nucl. Phys. **84** (1966) 673